ORNL/TM-2024/3455

Summary of FY2024 Experimental Results to Support Development of New Inelastic Material Models and Validation of Section III, Division 5, Class A Design Rules

Yanli Wang

July 2024

OAK RIDGE National Laboratory

ORNL IS MANAGED BY UT-BATTELLE LLC FOR THE US DEPARTMENT OF ENERGY

ORNL/TM-2024/3455

Materials Science and Technology Division

SUMMARY OF FY2024 EXPERIMENTAL RESULTS TO SUPPORT DEVELOPMENT OF NEW INELASTIC MATERIAL MODELS AND VALIDATION OF SECTION III, DIVISION 5, CLASS A DESIGN RULES

Yanli Wang

Date Published: July 2024

Prepared by
OAK RIDGE NATIONAL LABORATORY
Oak Ridge, TN 37831
managed by
UT-BATTELLE LLC
for the
US DEPARTMENT OF ENERGY
under contract DE-AC05-00OR22725

This page intentionally left blank

CONTENTS

This page intentionally left blank.

LIST OF FIGURES

LIST OF TABLES

ACKNOWLEDGMENTS

This research was sponsored by the United States (U.S.) Department of Energy (DOE) under Contract No. DE-AC05-00OR22725 with Oak Ridge National Laboratory (ORNL), which is managed and operated by the University of Tennessee– Battelle LLC. Programmatic direction was provided by the DOE Office of Nuclear Energy (NE).

The authors gratefully acknowledge the support provided by Sue Lesica, Federal Materials Lead for the DOE-NE Advanced Reactor Technologies (ART) Program, Matthew Hahn, Federal Program Manager of the ART Gas-Cooled Reactors (GCR) Campaign, and Gerhard Strydom of Idaho National Laboratory, National Technical Director of the ART GCR Campaign.

The authors also wish to thank ORNL staff members Bradley J Hall and C. Shane Hawkins for the technical support and Lianshan Lin and Zhili Feng for reviewing this report.

Special thanks are extended to Ting-Leung Sham of the U.S. Nuclear Regulatory Commission (NRC), who served as the Advanced Materials Technology Area Lead for the ART Program within DOE-NE and supported this work prior to joining the US-NRC in FY2024.

This page intentionally left blank.

ABSTRACT

To address the data gap crucial for updating existing viscoplastic constitutive material models for the Class A materials in the American Society of Mechanical Engineers (ASME) Boiler and Pressure Vessel Code, Section III, Division 5, High Temperature Reactors (ASME, 2023) for inelastic design analysis, Oak Ridge National Laboratory (ORNL) conducted experimental studies on Alloy 800H and Alloy 617 across a range of temperatures up to their maximum temperature limits in Section III, Division 5. The studies aim to characterize the materials' deformation behavior under both strain-controlled mechanical cyclic loading and thermal cycling conditions.

This report summarizes ORNL's FY 2024 experimental findings on Alloy 800H and Alloy 617, focusing on pure fatigue tests, cyclic stress-strain curves, thermomechanical fatigue experiments, and verification of the high temperature cyclic damage summation design rules.

1. BACKGROUND

The use of inelastic analysis methods represents the most accurate and least overly conservative approach among ASME high-temperature nuclear reactor design options. Under the Advanced Reactor Technologies (ART) Program, viscoplastic constitutive models have been developed for Grade 91 steel, Type 316 stainless steel, and Alloy 617 to facilitate their application in reactor design following the inelastic design rules outlined in the ASME Boiler and Pressure Vessel Code, Section III, Division 5, High Temperature Reactors (ASME, 2023), Subsection HB, Subpart B. Beginning in FY 2022, efforts commenced at Argonne National Laboratory (ANL) and Oak Ridge National Laboratory (ORNL) to develop a viscoplastic constitutive model for Alloy 800H, which is one of the six remaining Class A materials in Section III, Division 5. ORNL has been tasked with generating experimental data (Wang et al., 2022) to support the development of this material model. Currently, the Alloy 800H material model, formulated at ANL, is undergoing review and ballot by the ASME code committee.

While material models for the remaining Class A materials are still in development, the current formulations for Alloy 617, 316H, Grade 91, and Alloy 800H are distinct from each other. Based on feedback from ASME code committees, there is a recognized need to establish 'universal' model forms for all the Class A materials to facilitate easier implementation by designers. Recently, ANL has launched efforts to develop a new material model form aimed at streamlining the design process and enabling high-temperature reactor designers to effectively apply these models. In support of this initiative, ORNL is conducting experiments to validate the new material models and refine their parameters. This report provides a summary of the experiments conducted at ORNL during FY2024.

Additionally, Additionally, results from the experimental work performed to verify the high temperature damage summation design rules are briefly discussed and summarized.

2. MATERIALS AND EXPERIMENTAL

2.1 ALLOY 800H AND ALLOY 617 MATERIALS

Alloy 800H is an approved Class A material in the ASME code for nuclear applications up to 760°C with a maximum design life of 300,000 h. The Alloy 800H material used in this study had a Heat number of 37458 and was a historical reference plate material stored at ORNL. The plate, with nominal thickness of ½-inch, was manufactured by Jessop Steel Company in 1989 and has a factory marking of UNS 08811, which indicates that it meets the ASTM B409-87 specification, an earlier version of ASTM B409-06 specification.

The chemical composition of the Alloy 800H and the ASTM B409-06 specifications are listed in Table 1. The combined content of Al and Ti is 0.88 wt %, which meets the minimum requirements of 0.50 wt % per ASME Section III, Division 5 Table HBB-I-14.1(a). Additionally, Wright et al. (2010) performed detailed characterization of this heat of Alloy 800H and verified its compliance with the Alloy 800H specifications, including grain size and tensile properties.

Table 1. Chemical compositions of Alloy 800H (Heat number 37458) compared with the chemical requirements of ASTM B409-06 (wt %)

Alloy 800H	Heat No. 37458	ASTM 409B-06
Ni	30.45	30.0–35.0
Cr	19.3	19.0–23.0
Fe	47.05	39.5 min.
Mn	1.31	1.5 max.
C	0.063	0.06–0.10
Cu	0.21	0.75 max.
Si	0.37	1.0 max.
S	0.001	0.015 max.
Al	0.43	0.15–0.6
Ti	0.45	0.15–0.6
Mo	0.21	—
Co	0.11	—

The solution annealed hot-rolled Alloy 617 plate with Heat number 314626 from ThyssenKrupp VDM USA Inc was used to fabricate Alloy 617 test specimens for this study. This plate is one of the source materials used to generate the data package for the Alloy 617 code qualification as Class A component construction for high temperature reactors. The material plate has a nominal thickness of 1.75-inch. Table 2 lists the chemical composition of the Alloy 617 plate.

Table 2. Chemical compositions of the Alloy 617 plate with Heat number 314626 (wt%)

C	S	Cr	Mn	Si	Mo	Ti	Cu	Fe	Al	Co	B	Ni
0.05	<0.002	22.2	0.1	0.1	8.6	0.4	0.04	1.6	1.1	11.6	<0.001	balance

The specimen geometry for both alloys used in this report is shown in Figure 1. All the specimens were tested in their as-received condition. The Alloy 800H specimens were fabricated from the mid-thickness of the plate, whereas Alloy 617 specimens were machined at the ¼ thickness. The specimen longitudinal direction is oriented along the rolling direction of the material plate.

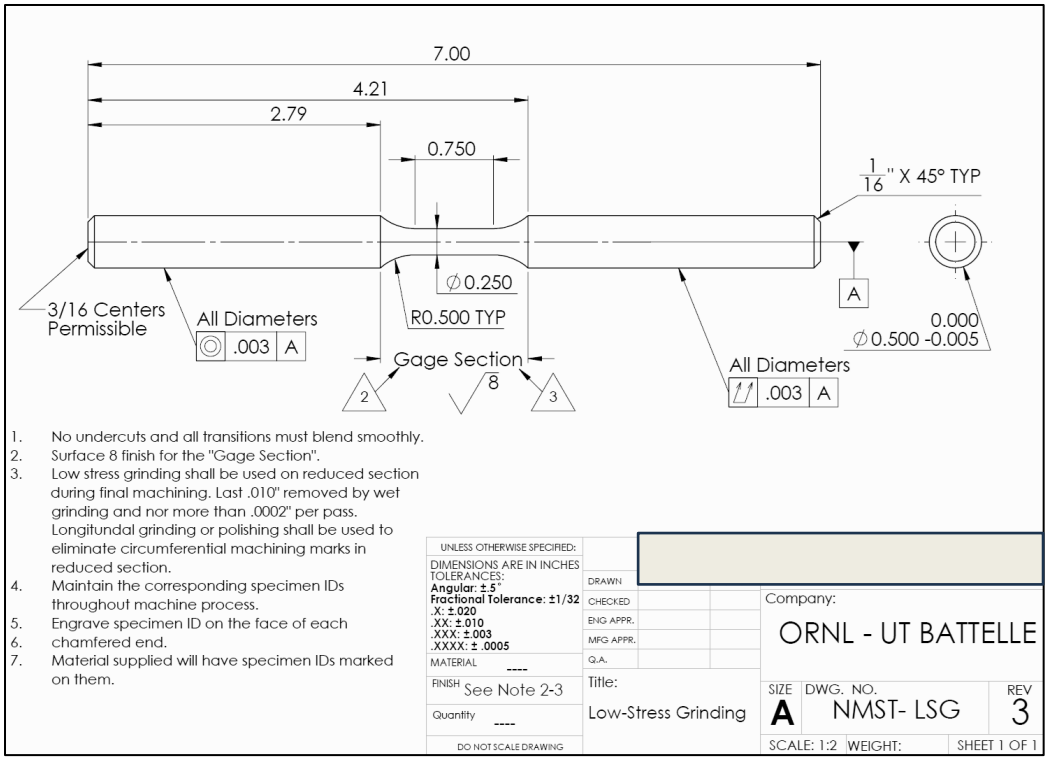

Figure 1. Standard fatigue and creep fatigue specimen geometry at Oak Ridge National Laboratory (ORNL). Dimensions are in inches.

2.2 FATIGUE AND CREEP-FATIGUE TESTING

Strain-controlled pure fatigue and creep-fatigue tests were conducted at various temperatures and followed the ASTM E606 standard. The strain rate was 1×10^{-3}/s. A triangular loading waveform with a fully reversed profile (i.e., loading ratio $R = -1$) was applied. The schematic of the loading profile for one cycle is presented in Figure 2. The control extensometer has a nominal gage length of ½-inch. For creep-fatigue, a hold time was applied to the peak tensile strain amplitude.

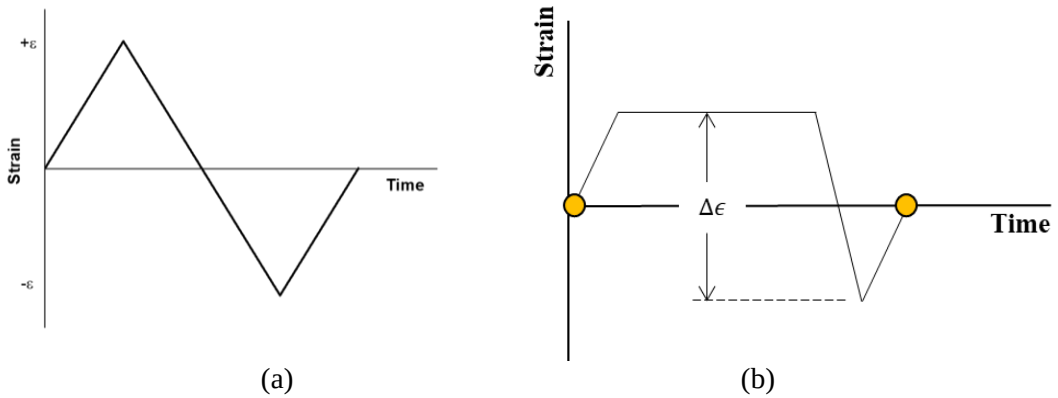

(a) (b)

Figure 2. Strain-controlled fatigue (a) and creep-fatigue (b) loading profile for one cycle.

While data from fatigue testing to steady state is generally adequate to assess the material deformation behavior and support material constitutive model development, fatigue tests were performed to failure whenever feasible, except for certain conditions at low strain ranges.

2.3 THERMOMECHANICAL FAITUGE TESTING

The thermomechanical fatigue experiments conducted on Alloy 617 and Alloy 800H are listed in Table 3. For each material, two temperature ranges were selected: one with testing temperature across the negligible creep to creep regime, and one within the creep region. The thermomechanical fatigue was conducted following the ASTM-2368 standard.

Table 3. Thermomechanical fatigue on Alloy 617 and Alloy 800H

Material	Specimen ID	Temperature range, ^{O}C	Heating cooling rate, ^{O}C/min	Notes
Alloy 617 (Heat no. 314626)	A617_R13TC1	350 to 950	30	Tested to failure (Wang, et al, 2018)
	A617_R23-BC3	700 to 900	30	Ongoing
Alloy 800H (Heat no. 37458)	A800H_10	450 to 760	30	Tested to failure
	A800H_2	550 to 650	30	Ongoing

The heating and cooling rates were 30^{o} C/min, resulting in a corresponding strain rate calculated to be approximately 8.3E-6/sec based on the thermal expansion coefficient and the heating and cooling rate of 30^{o}C/min. The temperature profile was automated and controlled by a LabView program.

The thermomechanical fatigue was under strain control with straining cycles that are 180 degrees out-of-phase with the thermal cycles. The total strain was controlled to be zero and the starting temperature was the mid-point of the thermal cycle, thus the applied strain ratio was -1.

Additional thermomechanical fatigue testing is planned and will cover the full temperature range for both materials, spanning from the lowest achievable temperature with the existing testing system up to the maximum temperature limits (950°C for Alloy 617 and 760°C for Alloy 800H). The results of these tests will be detailed in future reports.

3. EXPERIMENTS AND RESULTS

3.1 PURE FATIGUE TESTING ON ALLOY 800H

Strain controlled fatigue tests were performed at 23°C (room temperature) to 800°C. The nominal strain ranges include 0.3%, 0.4%, 0.6%, 0.75%, 0.8%, 1%, 1.5% and 2%. All the fatigue tests performed on Alloy 800H are listed in Table 4.

It is noted that most of the conditions were tested to failure, with a few exceptions at low strain range of 0.3% and 0.4%. The data with cycles to failure are presented on the nominal strain range versus cycles plot in Figure 3. The cycles to failure are defined at the 20% drop in the ratio of maximum to minimum stress. It is also noted that at large strain range of 2%, the specimens were often failed prematurely due to buckling, the available cycles are included in the plot as trend data. As test temperatures increase, the fatigue datasets demonstrate a trend shifting the fatigue curves towards lower values.

Table 4. Strain controlled fatigue testing for Alloy 800H (Heat number 37458)

ORNL TEST SEQUENCE NO AND ID	TEMPERATURE (°C)	NOMINAL STRAIN RANGE (%)	NOTES
800H_F33	RT	2	Tested to failure
800H_F44	RT	1	Tested to failure
800H_F31	RT	0.8	Tested to failure
800H_F48	RT	0.6	Tested to failure
800H_F14-01	RT	0.73	Tested to failure
800H_F47	RT	0.4	Tested to failure
800H_F19	RT	0.3	Interrupted
800H_F13-02	200	0.77	Tested to failure
800H_F12	350	2	Tested to failure
800H_F11	350	1	Tested to failure
800H_F29	350	0.8	Tested to failure
800H_F37	350	0.6	Tested to failure
800H_F46	350	0.4	Tested to failure
800H_F16-03	400	0.75	Tested to failure
A800H-7	450	1.5	Tested to failure
800H_F22	450	1	Tested to failure
800H_F17	450	0.8	Tested to failure
800H_F18	450	0.6	Tested to failure
800H_F35	450	0.4	Interrupted
800H_F25	550	2	Tested to failure
800H_F20	550	1	Tested to failure
800H_F16	550	0.8	Tested to failure
800H_F24	550	0.6	Tested to failure
800H_F38	550	0.4	Interrupted
800H_F15-04	600	0.75	Tested to failure
800H_F28	650	2	Tested to failure
800H_F21	650	1	Tested to failure
800H_F36	650	0.8	Tested to failure
800H_F32	650	0.6	Tested to failure
800H_F34	650	0.4	Tested to failure
800H_F17-05	700	0.74	Tested to failure
800H_F30	760	2	Tested to failure
800H_F45	760	2	Tested to failure
800H_F14	760	1	Tested to failure
800H_F15	760	0.8	Tested to failure
800H_F39	760	0.6	Tested to failure
800H_F41	760	0.4	Tested to failure
800H_F18-06	800	0.8	Tested to failure

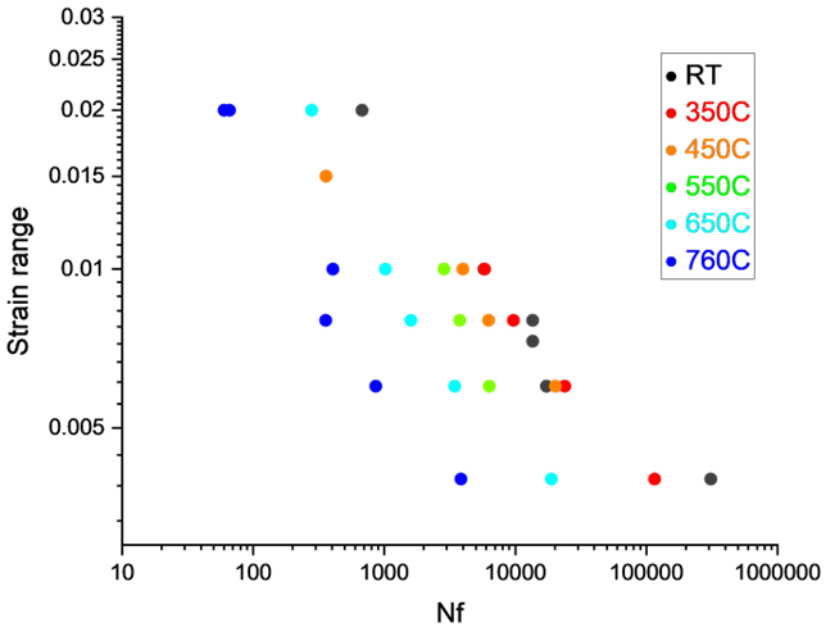

Figure 3. Strain controlled fatigue data on Alloy 800H.

For Alloy 800H at temperatures up to 800°F (425°C), a single fatigue design curve is provided for conditions below the creep region in ASME Section III, Division 5 (ASME, 2023), and then at temperatures of 540°C, 650°C and 760 °C. Note that these fatigue design curves are formulated based on the best-fit curves are determined as the lower of the two curves obtained with a reduction factor of two on the strain range and a reduction factor of twenty on the cycles to failure. Despite the absence of repeated tests or data from different heats of Alloy 800H to assess variability, and with available datasets at RT and 350°C viewed as one group, 550°C, 650°C and 760°C are shown to support the existing design fatigue curves in the ASME code (ASME, 2023).

3.2 CYCLIC STRESS-STRAIN CURVES FOR ALLOY 800H

The stress, strain, temperature, and loading time data for all cycles of these fatigue tests have been recorded and are available for use in calibrating the material model parameters. In this report, the peak stresses from these fatigue tests are presented, with Figures 4 to 9 plot the maximum and minimum stresses as a function of applied cycles for all fatigue tests conducted on Alloy 800H. These tests revealed cyclic hardening behavior, with varying cyclic hardening rates observed across different temperatures and strain ranges.

Figure 10 compares stress ranges versus cycles at strain ranges of 0.4% and 1% for different testing temperatures. Interestingly, the cyclic hardening behavior is notably different at between 350°C and 650°C, exhibiting much higher hardening rates after the initial cycles (around 10 cycles at 1% strain range and 100 cycles at 0.4% strain range). There appear to be two competing mechanisms responsible for the cyclic hardening and softening effects observed with increasing testing temperatures. For some cases, the stress ranges at higher temperatures even surpass those measured at room temperature. At the high testing temperature of 760°C, the softening mechanism is most pronounced, where it manifests as the lowest

stress ranges among all tested conditions. The mechanisms responsible for these different responses at different temperatures is beyond the scope of this study.

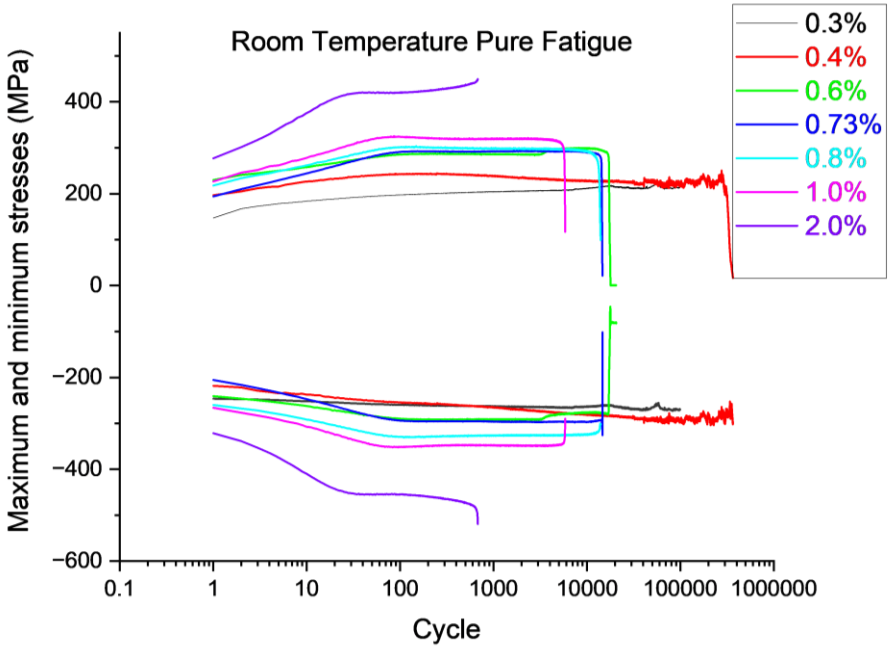

Figure 4. Maximum and minimum stresses as a function of applied cycle for fatigue testing on Alloy 800H at room temperature.

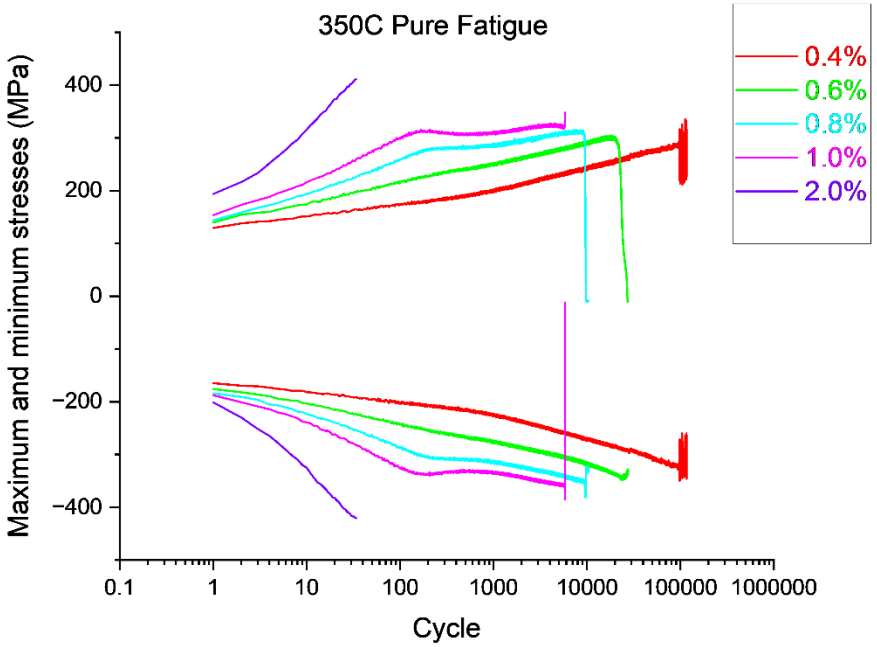

Figure 5. Maximum and minimum stresses as a function of applied cycle for fatigue testing on Alloy 800H at 350 ºC.

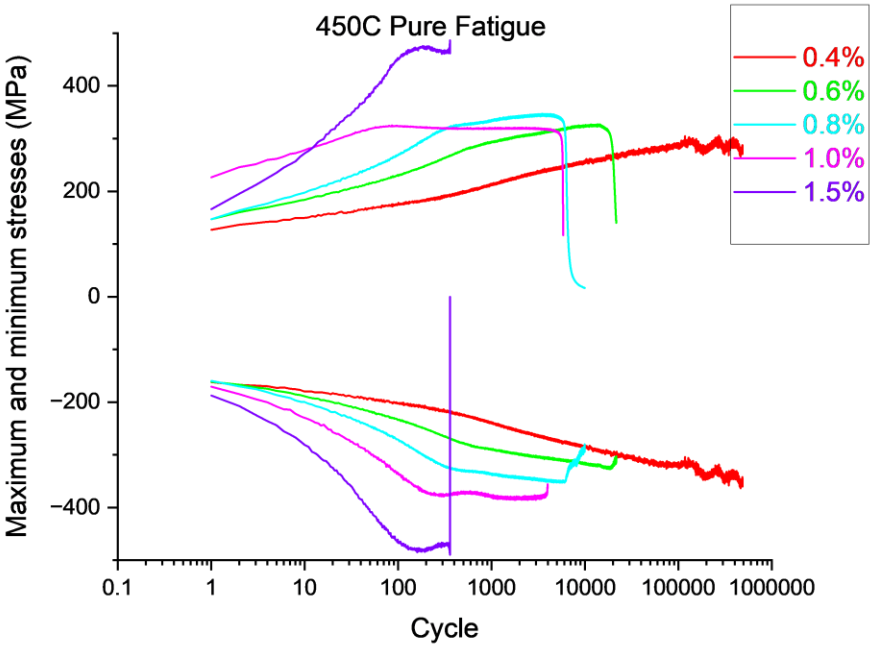

Figure 6. Maximum and minimum stresses as a function of applied cycle for fatigue testing on Alloy 800H at 450 ºC

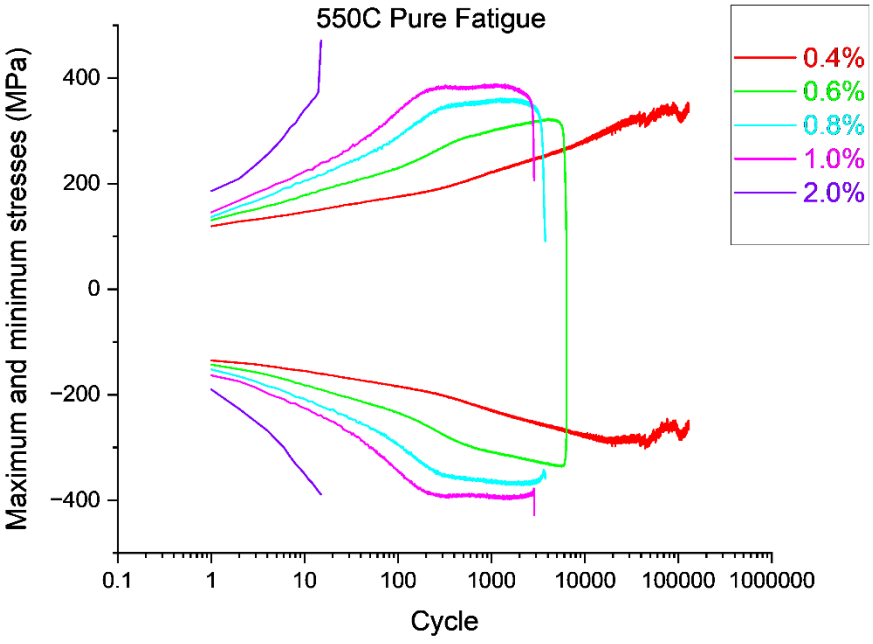

Figure 7. Maximum and minimum stresses as a function of applied cycle for fatigue testing on Alloy 800H at 550 ºC

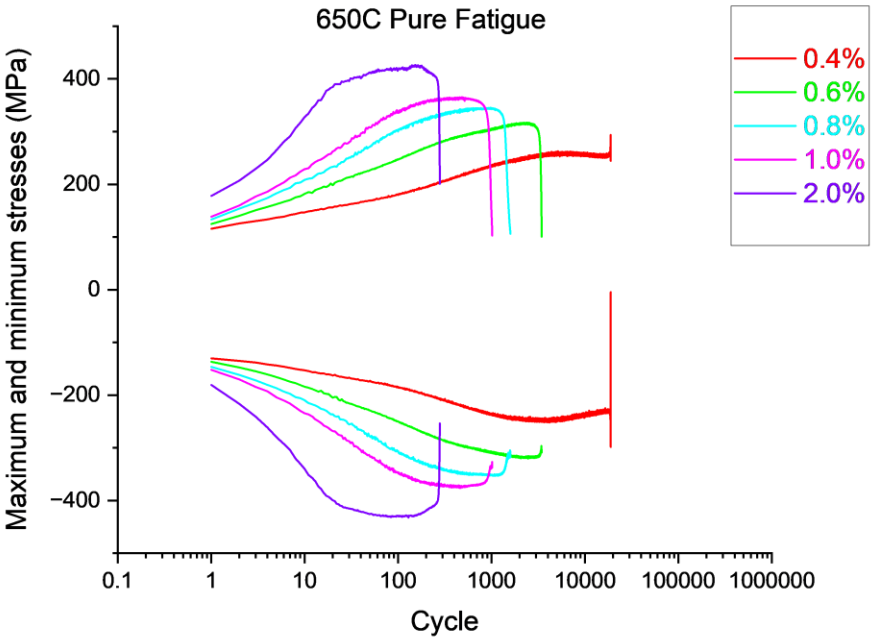

Figure 8. Maximum and minimum stresses as a function of applied cycle for fatigue testing on Alloy 800H at 650 ºC

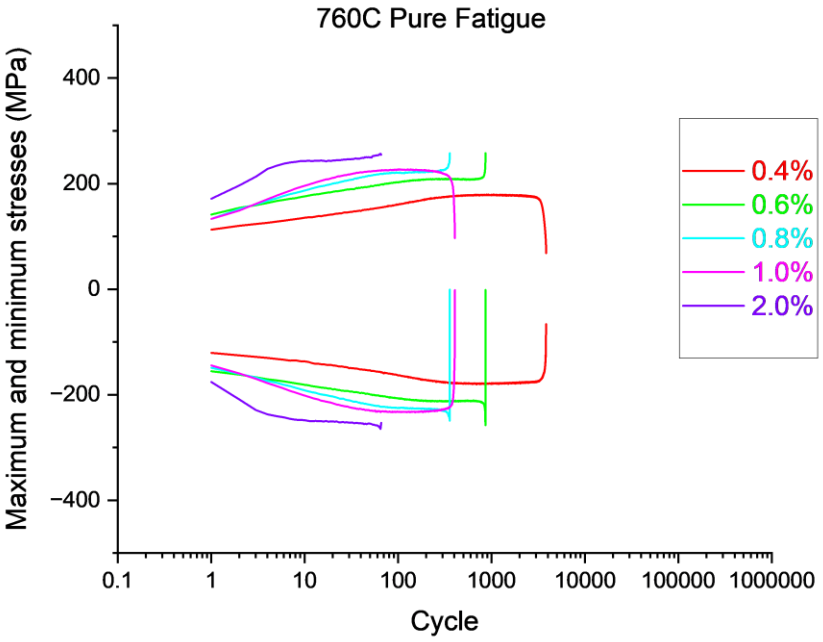

Figure 9. Maximum and minimum stresses as a function of applied cycle for fatigue testing on Alloy 800H at 760 ºC

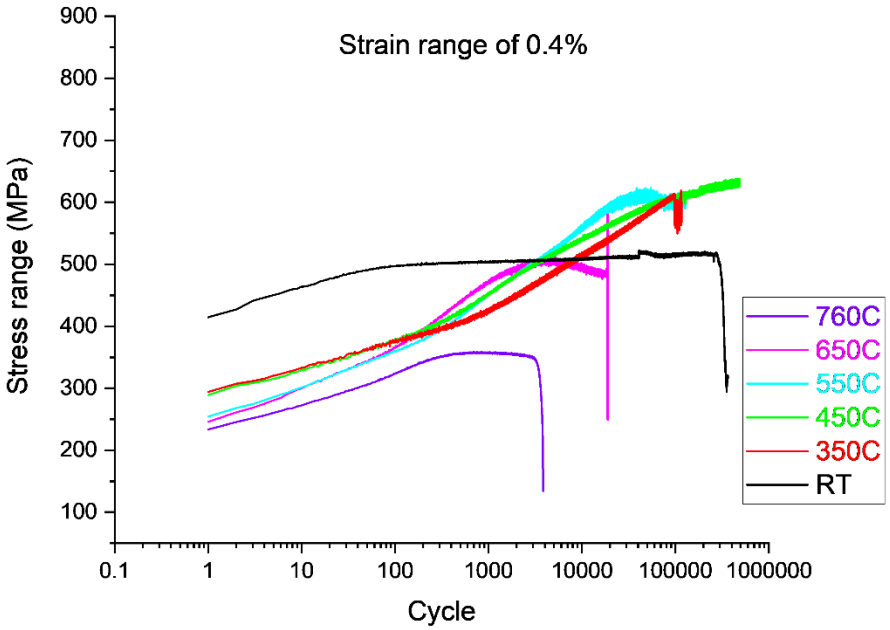

(a)

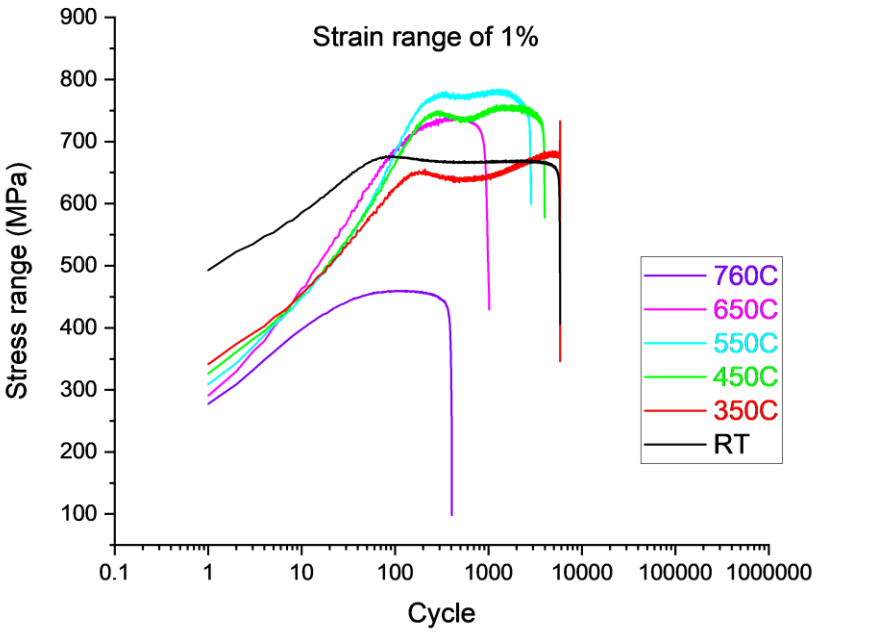

(b)

Figure 10. Stress range as a function of applied cycle for fatigue testing on Alloy 800H at 0.4% strain range (a) and 1% strain range (b)

The cyclic stress-strain curves of Alloy 800H at various testing temperatures were derived from the pure fatigue data. Stress ranges were calculated for each cycle, and these results are presented in Figure 11 for the representative cycles. As previously discussed, due to continuous cyclic hardening behavior observed between 350°C and 650°C, the cyclic stress-strain curves did not reach saturation until more than 500 cycles were applied to the test specimens. In contrast, at room temperature and high testing temperature of 760°C, saturation of the cyclic curves occurred after approximately 50 cycles, much earlier than in the intermediate temperature range.

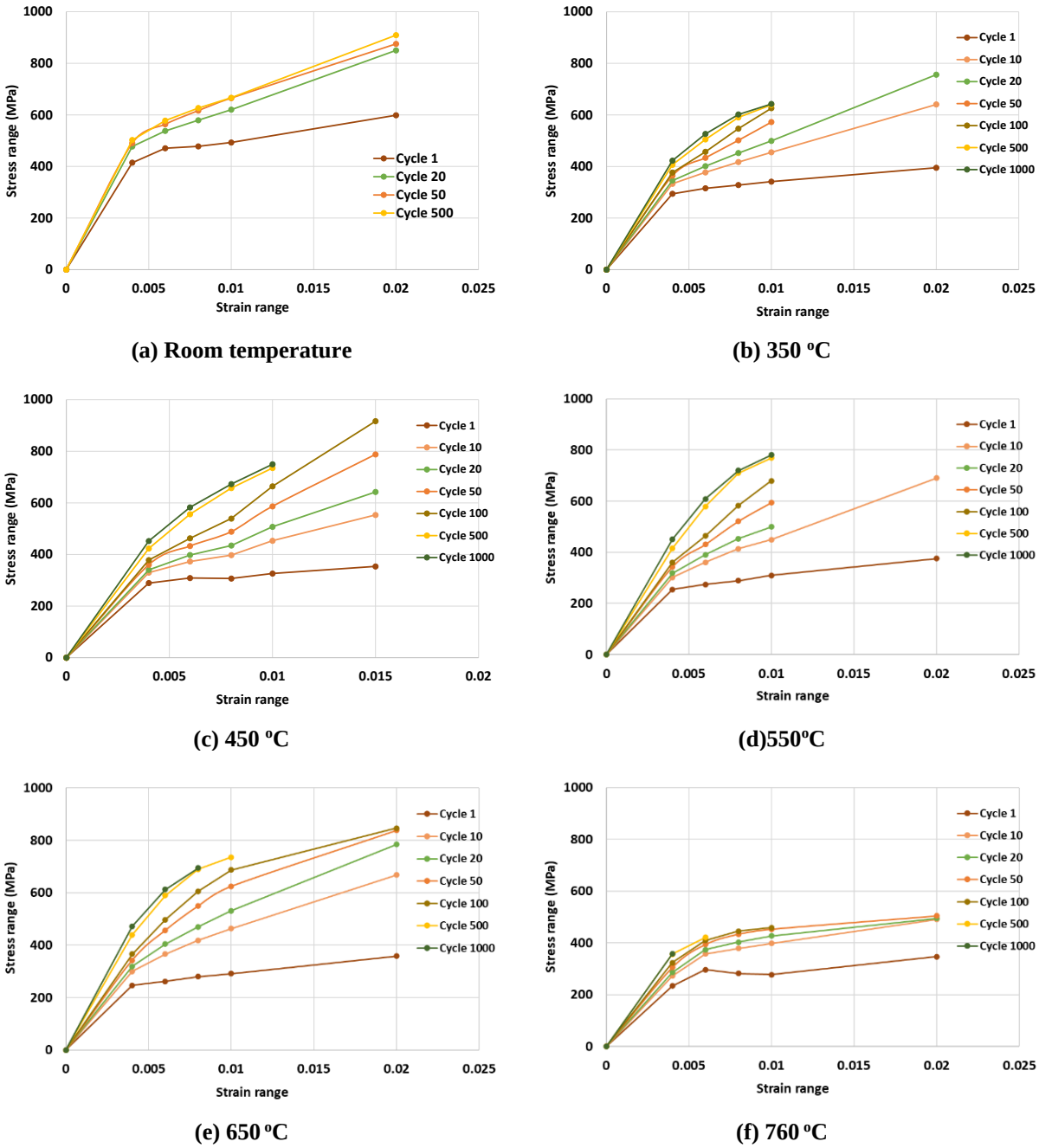

Figure 11. Alloy 800H cyclic stress-strain curves generated from the fatigue tests.

3.3 PURE FATIGUE TESTING ON ALLOY 617

To probe the material's mechanical response to cyclic loading at different strain ranges and temperatures while supporting the material parameters for the development of the viscoplastic constitutive model, pure fatigue loading experiments were designed and performed to collect key experimental information at selected strain ranges (i.e., 0.4%, 0.6%, 0.8%, 1.0% and 2%) at temperatures of 400°C 500°C, 600°C, 700°C and 800°C.

It is noted that most of the conditions were tested to failure except for a few tests at low strain range of 0.4%. The data with cycles to failure are presented on the nominal strain range versus cycles plot in Figure 12. The cycles to failure are defined at the 20% drop in the ratio of maximum to minimum stress. As test temperatures increase, the fatigue datasets demonstrate a trend shifting the fatigue curves towards lower values.

Table 5. Strain controlled fatigue testing for Alloy 617 (Heat number 314626)

ORNL Test ID	Temperature (°C)	Nominal Strain Range (%)	Notes
A617_R27-AD5	400	2	Tested to failure
A617_R12TC2-2013	400	1	Tested to failure
A617_R27-AD4	400	0.8	Tested to failure
A617_R5-BC3	400	0.6	Tested to failure
A617_R27-AC1	400	0.4	Interrupted
A617_R27-AC4	500	2	Tested to failure
A617_R27-AD7	500	1	Tested to failure
A617_R26-BC3	500	0.8	Tested to failure
A617_R26-BC4	500	0.6	Tested to failure
A617_R25-BC6	500	0.4	Interrupted
A617_R27-AD2	600	2	Tested to failure
A617_R13TC9-2014	600	1	Tested to failure
A617_R27-AC2	600	0.8	Tested to failure
A617_R27-AD6	600	0.6	Tested to failure
A617_R27-AC3	600	0.4	Interrupted
A617_R27-AC7	700	2	Tested to failure
A617_R27-AC8	700	1	Tested to failure
A617_R27-AD1	700	0.8	Tested to failure
A617_R27-AD8	700	0.6	Tested to failure
A617_R27-AC5	700	0.4	Tested to failure
A617_R23-BC5	800	2	Tested to failure
A617_R12TC8-2105	800	1	Tested to failure
A617-R26-BC-5	800	0.8	Tested to failure
A617-R26-BC-4	800	0.6	Tested to failure
A617-R23-TC-5	800	0.4	Tested to failure

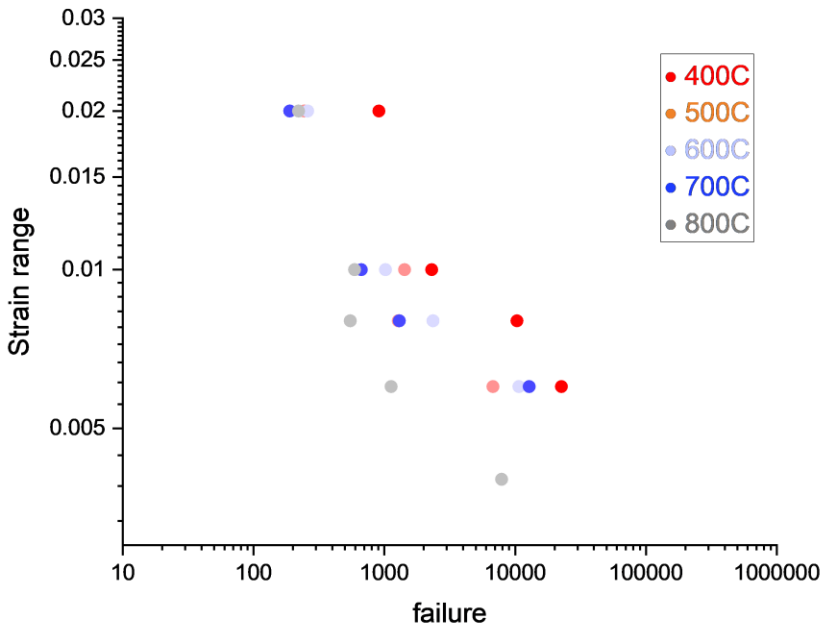

Figure 12. Strain controlled fatigue data on Alloy 617.

3.4 CYCLIC STRESS-STRAIN CURVES FOR ALLOY 617

The stress, strain, temperature, and loading time data for all cycles of these fatigue tests have been recorded and are available for use in calibrating the material model parameters. In this report, the peak stresses from these fatigue tests are presented, with Figures 13 to 17 plot the maximum and minimum stresses as a function of applied cycles for all fatigue tests conducted on Alloy 617, and these tests revealed cyclic hardening behavior, with similar cyclic hardening rates observed across different temperatures at the same strain ranges, different than Alloy 800H.

Figure 18 compares stress range versus applied cycles at strain ranges of 0.4% and 1% for different testing temperatures. It is evident that at both strain ranges at 400 and 500 °C, the material showed similar slopes for the stress range versus cycle curves, indicating no significant differences in the cyclic hardening rates or cyclic hardening mechanisms at these temperatures. However, at the 0.4% strain range, starting at 600°C, the material deformation mechanism likely shifted, as the initial loading resulted in higher stresses compared to lower temperatures. This phenomenon is not observed at the larger strain range of 1%, where the cyclic hardening rates show distinct groupings at 400°C/500°C, 600°C/700°C, and 800°C.

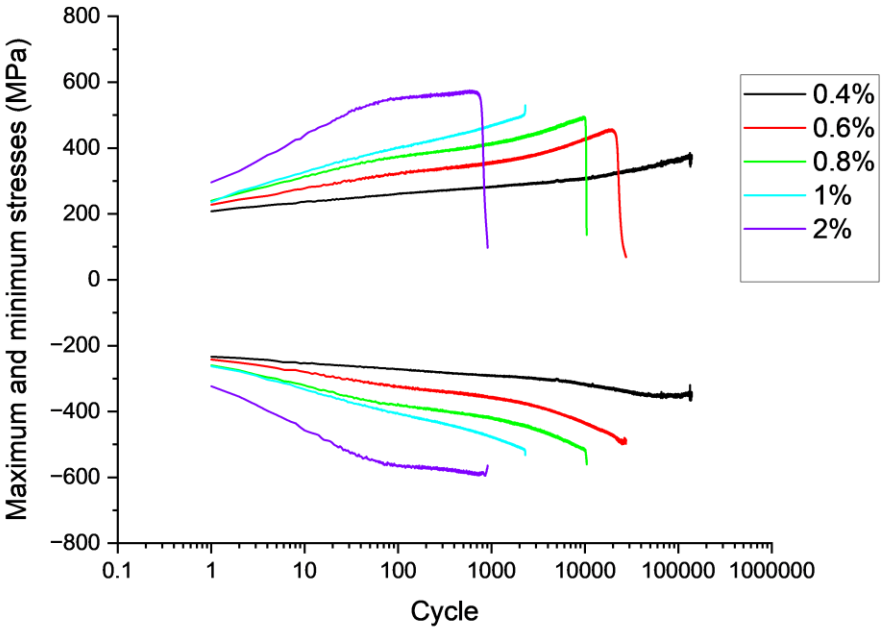

Figure 13. Maximum and minimum stresses as a function of applied cycle for fatigue testing on Alloy 617 at 400 ºC.

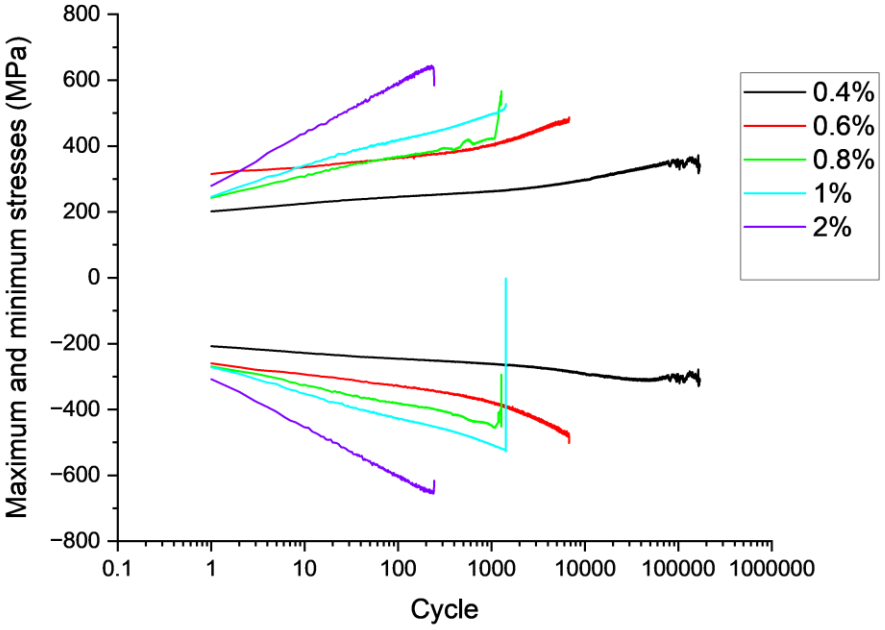

Figure 14. Maximum and minimum stresses as a function of applied cycle for fatigue testing on Alloy 617 at 500 ºC.

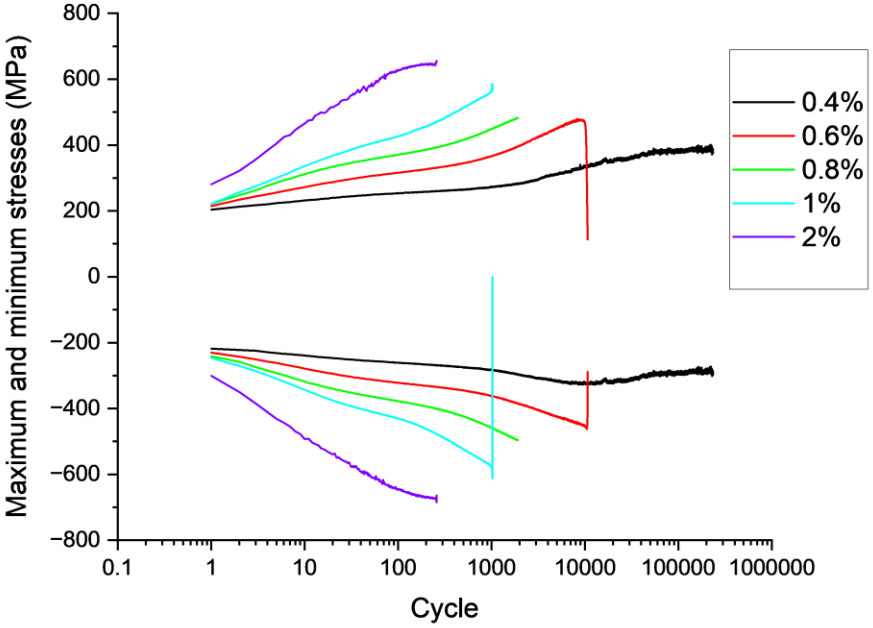

Figure 15. Maximum and minimum stresses as a function of applied cycle for fatigue testing on Alloy 617 at 600 ºC.

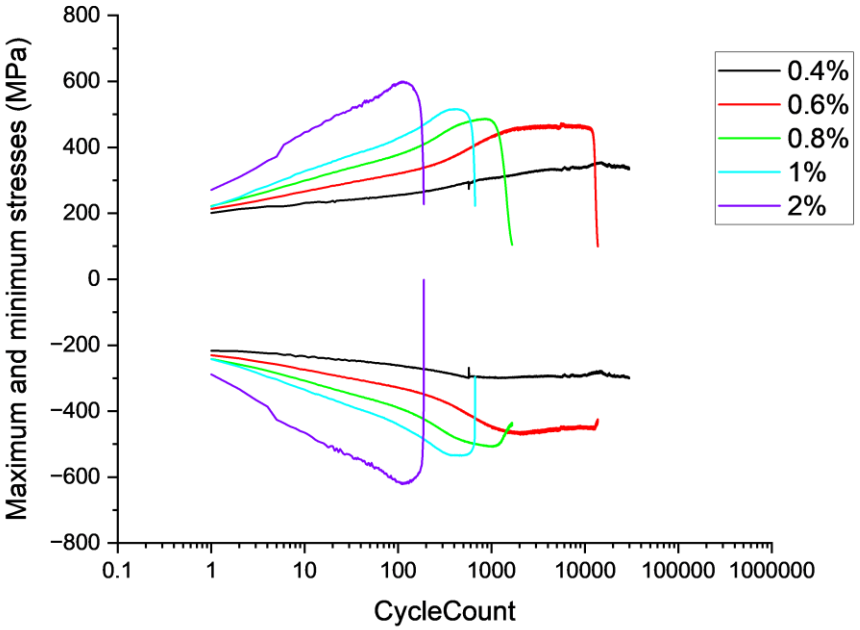

Figure 16. Maximum and minimum stresses as a function of applied cycle for fatigue testing on Alloy 617 at 700 ºC.

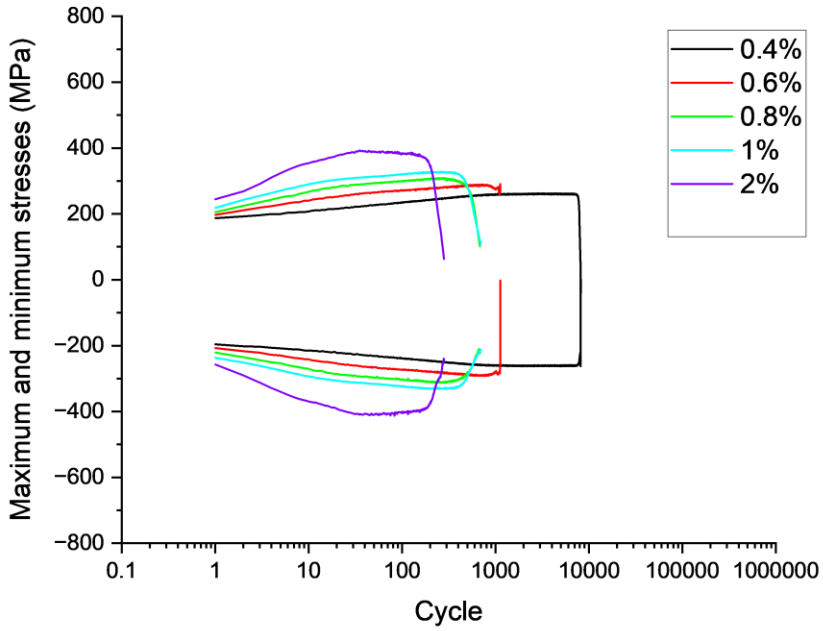

Figure 17. Maximum and minimum stresses as a function of applied cycle for fatigue testing on Alloy 617 at 800 ºC.

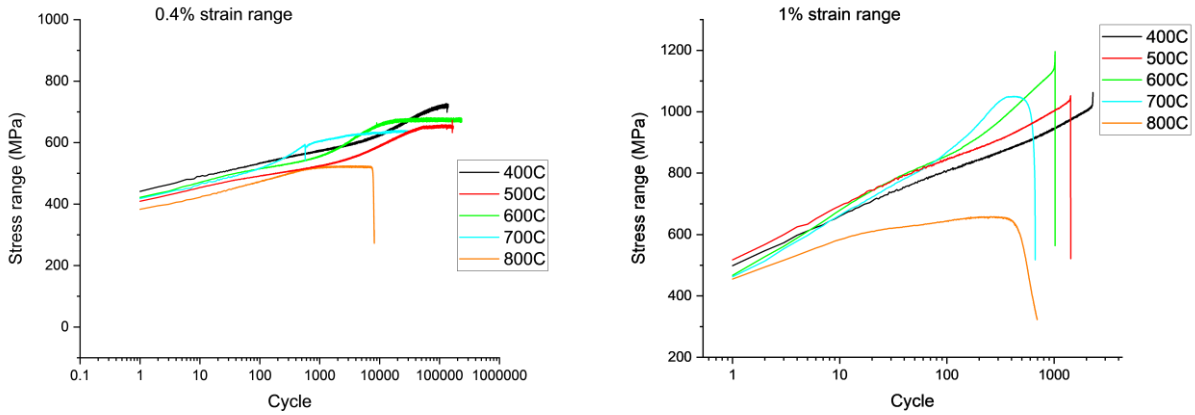

(a) **(b)**

Figure 18. Stress range as a function of applied cycle for fatigue testing on Alloy 617 at 0.4% strain range (a) and 1% strain range (b)

The cyclic stress-strain curves of Alloy 617 at the testing temperatures were derived from pure fatigue data, as shown in Figure 19 for representative cycles. Continuous cyclic hardening behavior was observed between 400°C and 700°C, preventing the cyclic stress-strain curves from reaching saturation, even after 1000 applied cycles. In contrast, at the highest test temperature of 800°C, saturation of the cyclic curves occurred after approximately 50 cycles.

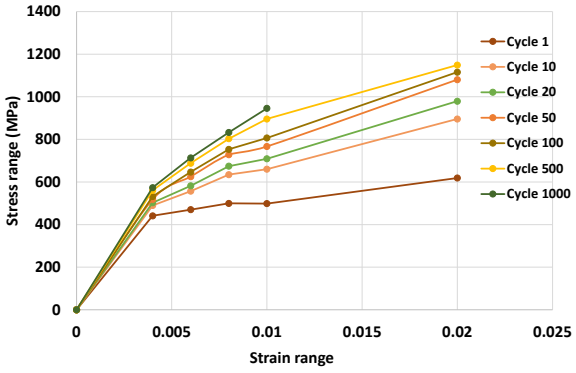

(a) 400 °C

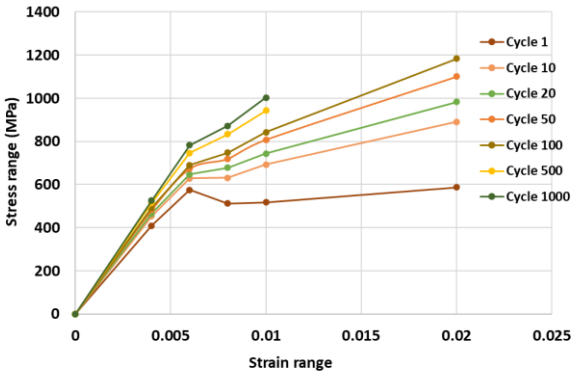

(b) 500 °C

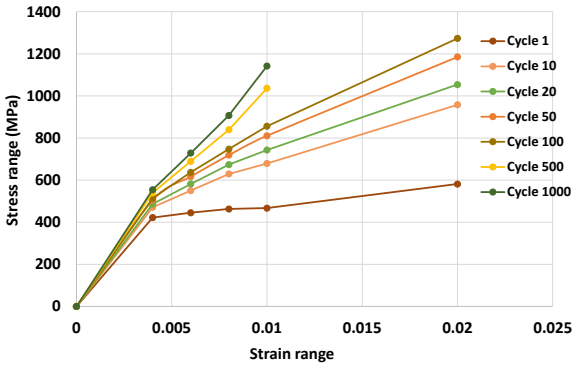

(c) 600 °C

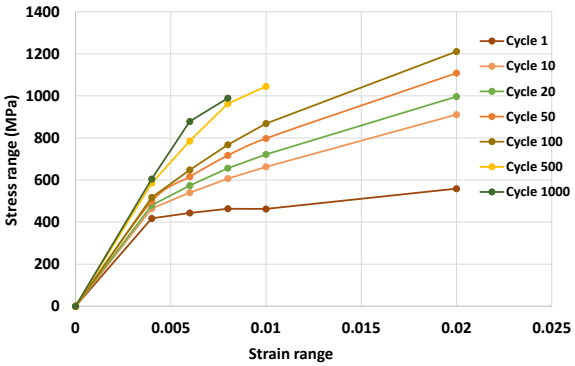

(d) 700 °C

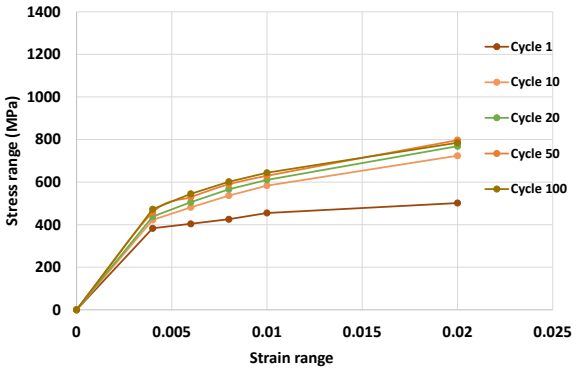

(e) 800 °C

Figure 19. Alloy 617 cyclic stress-strain curves generated from the fatigue tests.

3.5 THERMOMECHANICAL FATIGUE TESTING OF ALLOY 800H AT TEMPERATURE RANGES OF 450 TO 760°C AND 550 TO 650°C

Thermomechanical fatigue testing on Alloy 800H was conducted in two temperature ranges: from 450 to 760°C, which was tested to failure, and from 550 to 650°C, which is currently ongoing at the time of writing this report. The available results are summarized below.

The mechanical strain is calculated by subtracting the thermal expansion from the total strain. The thermal expansion coefficient (CTE) of an average value of 16.6E-6 mm/mm/ ^{o}C were used for the calculation of the mechanical strain, and the strain range was 0.51% and 0.17% for the two temperature ranges, respectively. The experimentally measured thermal cycle and mechanical strain history in one thermal cycle are plotted in Figure 20. The maximum and minimum stresses and stress range are plotted Figure 21, and representative hysteresis loops are plotted in Figure 22.

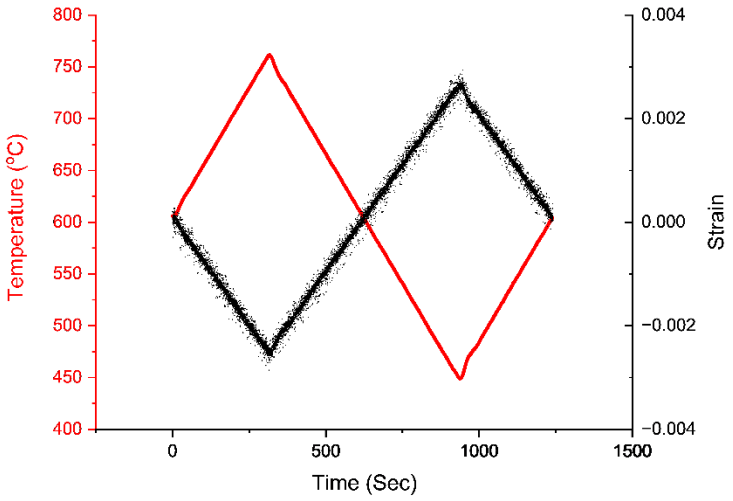

(a)

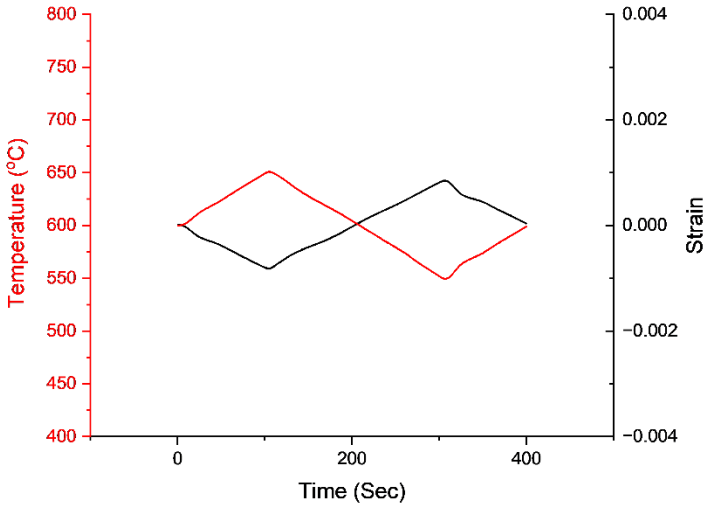

(b)

Figure 20. Temperature and mechanical strain history of one thermal cycle for thermomechanical testing on Alloy 800H at 450 to 760ºC (a) and 550 to 650 ºC (b)

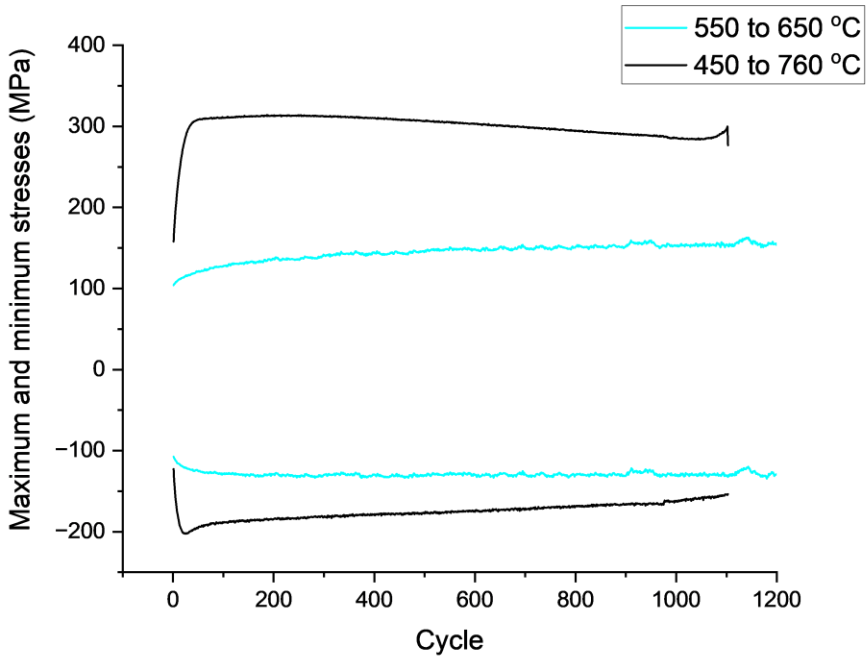

(a)

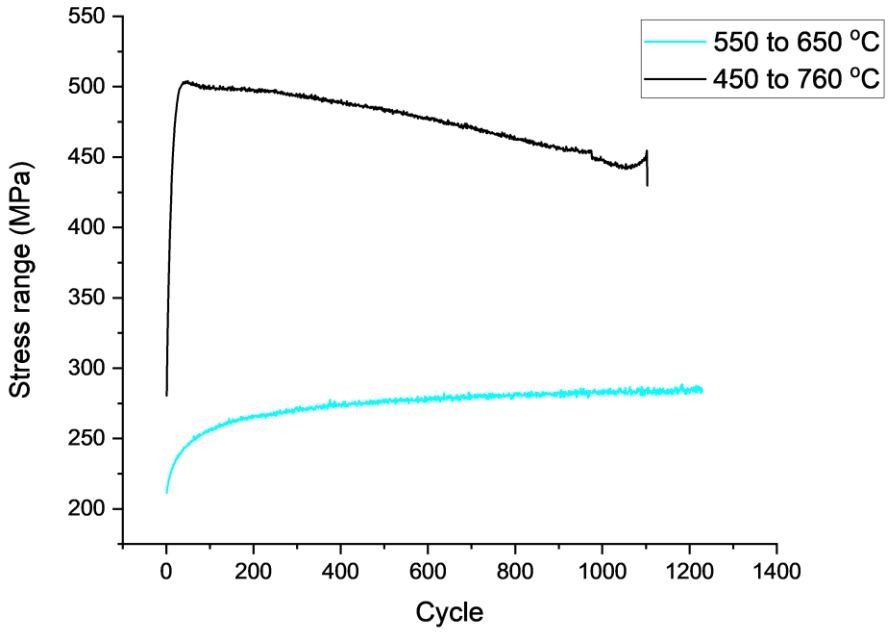

(b)

Figure 21. Alloy 800H thermomechanical fatigue at temperature range of 450 to 760° C and 550 to 650 °C with maximum and minimum stresses (a) and stress range (b).

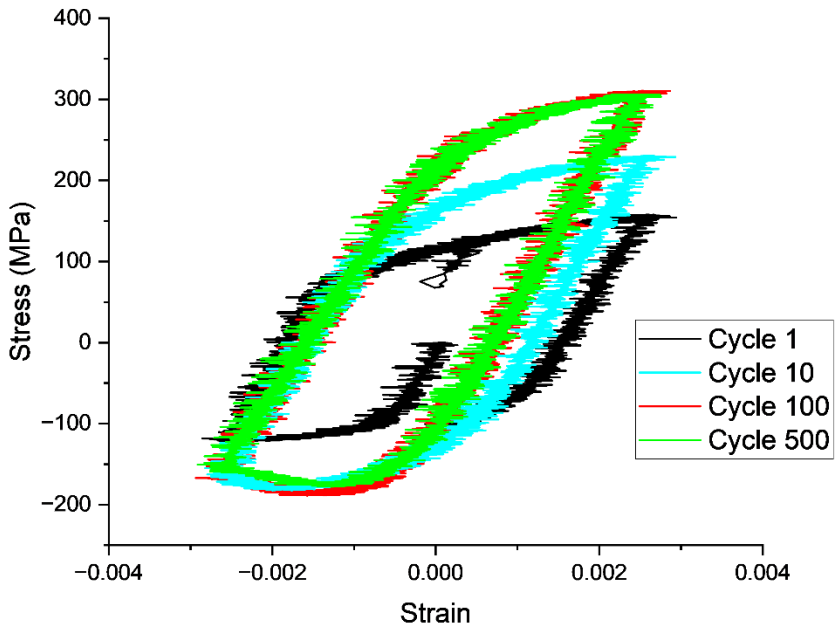

(a)

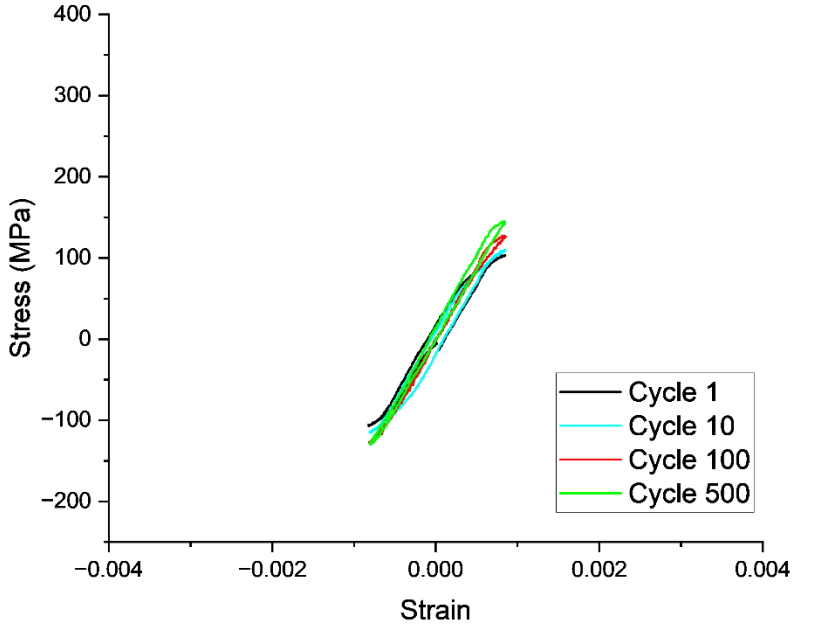

(b)

Figure 22. Representative hysteresis loops of the thermomechanical fatigue at temperature ranges of 450 to 760° C (a) 550 to 650° C (b) on Alloy 800H

For the experiment conducted at 450 to 760°C, the specimen was tested to failure, which occurred after 1103 cycles. Initially, the specimen exhibited cyclic hardening behavior for approximately 50 cycles, after which it transitioned into a steady-state softening phase. This behavior is clearly illustrated by the plots of maximum and minimum stresses, as well as stress range as a function of applied cycles. As the material cyclic hardened, the inelastic strain range progressively decreased, shown from the decreasing width of the hysteresis loops.

The experiment conducted at 550 to 650°C showed continuous cyclic hardening throughout the entire applied cycles. The inelastic strain range decreased as more thermal cycles were applied, clearly illustrated by the hysteresis loops shrinking to nearly complete elastic after 500 cycles.

3.6 THERMOMECHANICAL FATIGUE TESTING OF ALLOY 617 AT TEMPERATURE RANGES OF 350 TO 950°C AND 700 TO 900°C

Thermomechanical fatigue testing on Alloy 617 at the temperature range of 350 to 950°C was previously completed and tested to failure (Wang, et al, 2018). A new experiment is ongoing at the temperature range of 700 to 900°C in this reporting period. The available results from these two tests are compared below.

The mechanical strain is calculated by subtracting the thermal expansion from the total strain. The thermal expansion coefficient (CTE) of an average value of 16.5E-6 mm/mm/ ^{o}C were used for the calculation of the mechanical strain, and the strain range was 1% and 0.33% for the two tests at the two temperature ranges, respectively. The experimentally measured thermal cycle and the calculated mechanical strain histories in one thermal cycle are plotted in Figure 23. The maximum and minimum stresses and stress range are plotted Figure 24, and hysteresis loops of cycle 1 and cycle 100 are plotted in Figure 25.

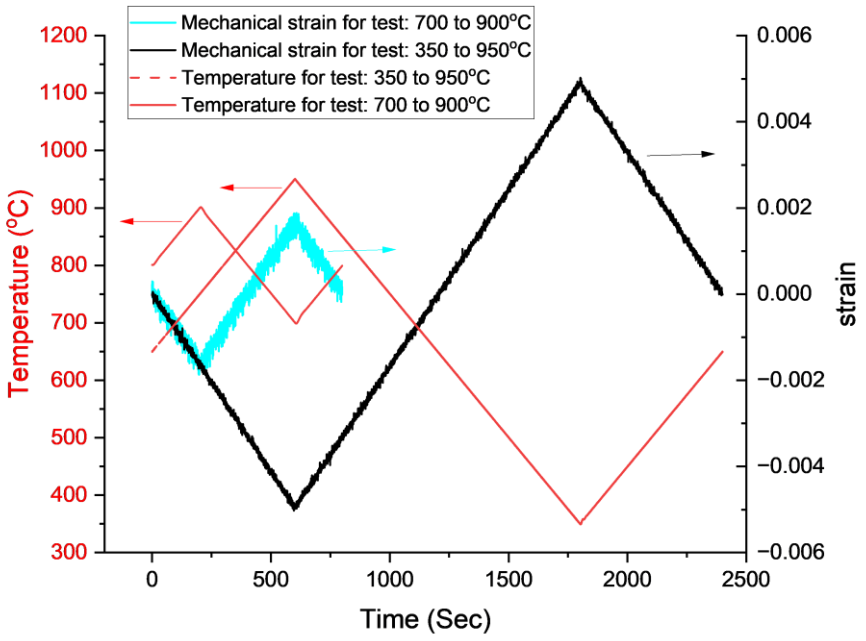

Figure 23. Temperature and mechanical strain history of one thermal cycle for thermomechanical testing on Alloy 617 at 350 to 950°C and 700 to 900 °C

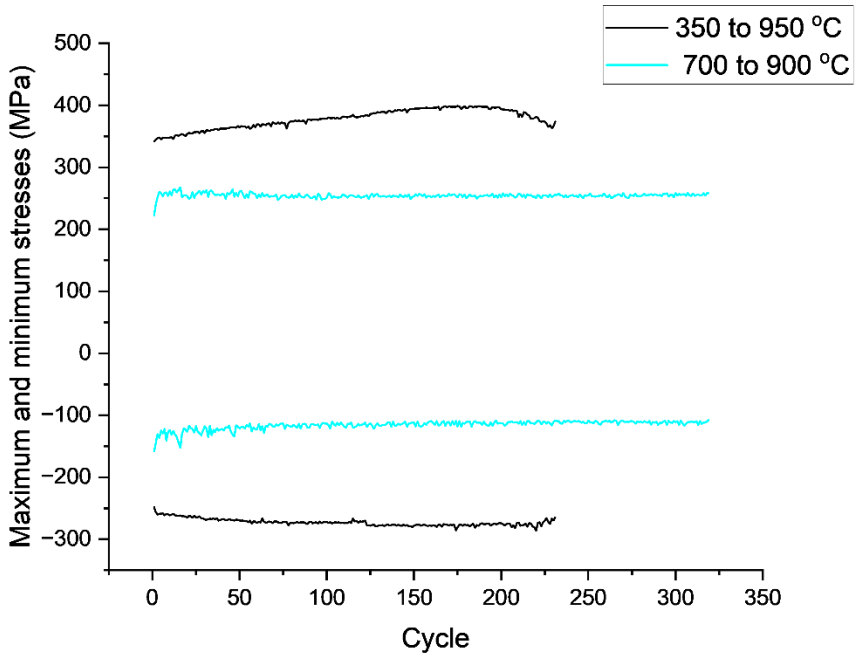

(a)

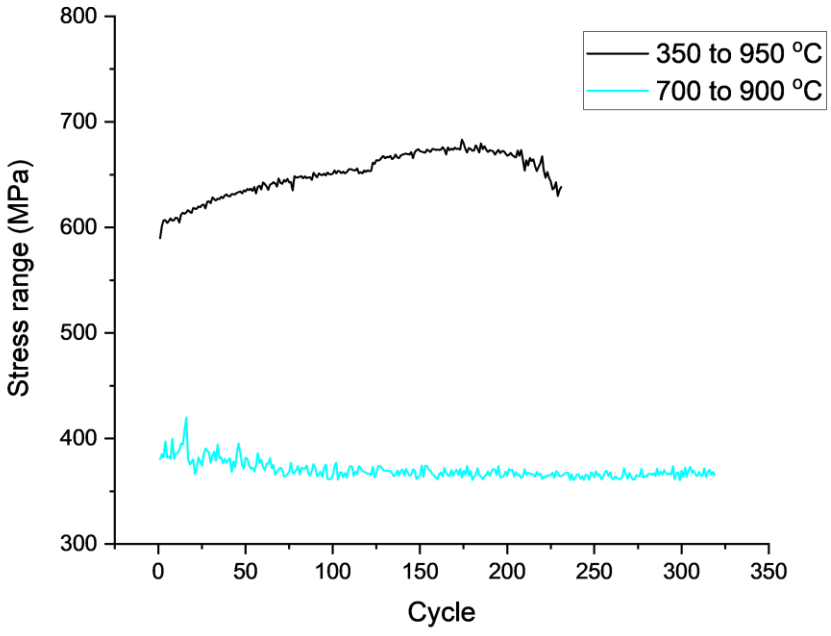

(b)

Figure 24. Alloy 617 thermomechanical fatigue at temperature range of 350 to 950° C and 700 to 900 °C with maximum and minimum stresses (a) and stress range (b).

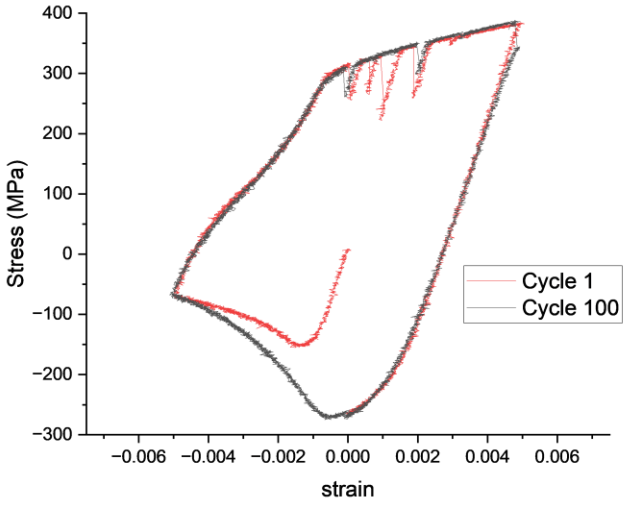

(a)

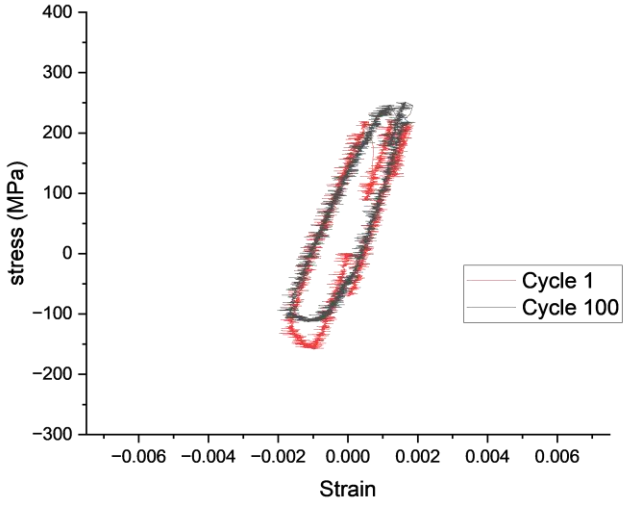

(b)

Figure 25. Hysteresis loops of the cycle 1 and cycle 100 of the thermomechanical fatigue at temperature ranges of 350 to 950ºC (a) and 700 to 900 ºC (b) on Alloy 617

For the experiment conducted at the temperature range of 350 to 950°C, the number of cycles to failure was 231. The specimen exhibited cyclic hardening behavior till failure initiation at about 180 cycles. This behavior is clearly illustrated by the plots of maximum and minimum stresses, as well as stress range as a function of applied cycles. The experiment conducted at the temperature range of 700 to 900°C showed saturation after the initial cycles.

Both tests on Alloy 617 showed serrated yielding behavior. Shown on the stress versus temperature plots in Figure 26, this serrated yield phenomenon was affected by the testing temperature range, and it was

pushed the onset temperature from 740°C to 700°C when the testing temperature range was increased. The mechanisms responsible for the serrated yield phenomenon is beyond the scope of this study.

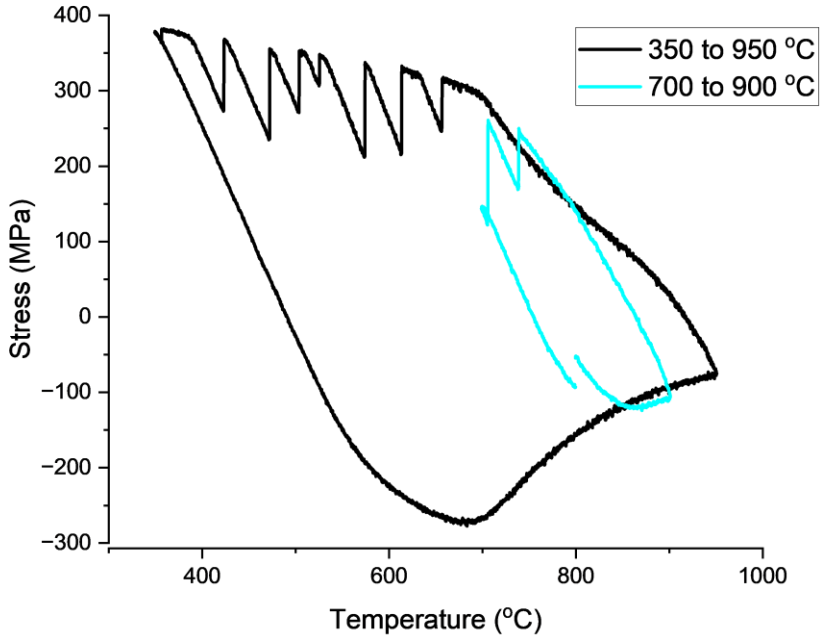

Figure 26. Stress versus temperature profiles of the cycle 10 in the thermomechanical tests on Alloy 617

4. EXPERIMENTAL AND ANALYTICAL VERIFICATION OF ASME SECTION III, DIVISION 5 CREEP-FATIGUE DESIGN RULES

In ASME Section III, Division 5, for a design to pass the creep-fatigue acceptance criteria, creep damage and fatigue damage are evaluated separately, and these damages must not violate the bi-linear creep-fatigue interaction diagram, i.e., the so-called D-diagram. The creep-fatigue damage evaluation procedure assumes that the effects of the actual cyclic loading sequence can be bounded by assuming that the individual loading cycles are uniformly distributed throughout the component design life.

In this FY2024, creep-fatigue experiments with variable amplitudes and loading sequencies were designed and performed on Alloy 617 at high 850 °C. The results were analyzed to evaluate the loading history effect on creep-fatigue damage accumulation and to verify the assumptions for the creep-fatigue evaluation design rules. The results were summarized in Wang et al (2024), and only briefly summarized here.

There were total of five creep-fatigue tests with multi-cycle types in the straining profile were performed on Alloy 617 at 850 °C. The two cycle types were one with 1% strain and a 600-second tension hold, and the second one with a 0.3% low strain range, also with a 600-second tension hold. The five tests are outlined below:

- Test **M1** has two segments: CF damage at 1% for 251 cycles followed by CF at 0.33% for 551 cycles to failure.

- Test **M2** has two segments: CF damage at 0.33% for 1600 cycles followed by CF at 1% for 35 cycles to failure.
- Test **M3** has two segments: CF damage at 0.33% for 824 cycles followed by CF at 1 % for 190 cycles to failure.
- Test **M4** has two segments**:** CF damage at 1% for 100 cycles followed by CF at 0.33% for 1344 cycles to failure.
- Test **M5** utilized a composite cycle for cycling. Each composite cycle unit consisted of 16 cycles at an average 0.18% strain range followed by 5 cycles at 1.16% strain range. The composite cycle unit was repeated till failure occurred.

It is noted that test M5 had the most complex straining profile, involving intermittent switching between high and low strain ranges. However, the strain amplitude was not well controlled, showing an average of 0.18% for the low strain range instead of the target 0.3%. The total CF damage fraction, defined as the ratio of the number of applied CF cycles to the failure cycles of that CF test under the same condition, were calculated for the five tests, and the results summarized in Table 6.

Table 6. Multi-cycle type creep-fatigue experiments on Alloy 617 at 850°C for verification of damage summation rules.

Test No.	**Strain range and number of cycles for each segment**	**CF fraction,** D_{cf}^{k}
M1	Seg.1. 1% for 251 cycles Seg.2. 0.33% for 551 cycles to failure	Seg.1. ~67% Seg.2. ~31% **Total: 98%**
M2	Seg.1. 0.33% for 1600 cycles Seg.2. 1% for 35 cycles to failure	Seg.1. ~90% Seg.2. ~9% **Total: 99%**
M3	Seg.1. 0.33% for 824 cycles Seg.2. 1% for 190 cycles to failure	Seg.1. ~46% Seg.2. ~50% **Total: 96%**
M4	Seg.1. 1% for 100 cycles Seg.2. 0.34% for 1344 cycles to failure	Seg.1. ~26% Seg.2. ~76% **Total: 102%**
M5	• 75 Composite cycle with (16 cycles at 0.2% followed by 5 cycles at 1.16%) • additional 16 cycles at 0.2% to failure	• 75 x (0.16%+1.3%) • additional 0.16% **Total: ~110%**

The results show that all five multi-cycle type tests exhibited total CF fractions within 100±10%, despite significant variations in strain profile, straining sequence, and the applied CF damage fraction at the initial segment. Additionally, the distribution of different cycle types in a design problem does not significantly affect the CF damage analysis results at elevated temperatures.

5. SUMMARY

In support of developing new viscoplastic constitutive models for inelastic analysis methods in Section III, Division 5 of the ASME Boiler and Pressure Vessel Code, experiments were conducted at ORNL to evaluate the mechanical responses of Alloy 800H and Alloy 617. Pure fatigue tests were performed over a temperature range from room temperature to 760°C on Alloy 800H, and from 400°C to 800°C on Alloy 617 to assess their cyclic responses. Cyclic stress-strain curves were generated for both materials at these test temperatures.

Thermomechanical fatigue tests were conducted at temperatures ranging from 450°C to 760°C and 550°C to 650°C on Alloy 800H, and from 350°C to 950°C and 700°C to 900°C on Alloy 617. These results were generated used to calibrate the temperature-dependent parameters in the constitutive models for the two materials.

Additionally, multi-cycle creep-fatigue experiments were performed on Alloy 617 to verify ASME Section III, Division 5 design rules. The findings indicate that the distribution of different cycle types does not significantly affect the creep-fatigue damage analysis results at 850°C.

REFERENCES

ASME. 2023. *Boiler and Pressure Vessel Code, Section III Division 5, Rules for Construction of Nuclear Facility Components, Subsection HB Subpart B,* American Society of Mechanical Engineers, New York (2023 Edition).

ASTM B409-06. 2016. *Standard Specification for Nickel-Iron-Chromium Alloy Plate, Sheet, and Strip*, ASTM International, West Conshohocken, Pennsylvania, www.astm.org.

ASTM E606/E606M-21. 2021. *Standard Test Method for Strain-Controlled Fatigue Testing*, ASTM International, West Conshohocken, Pennsylvania, www.astm.org.

Wright, J. K., Wright, R. N., and Sham T.-L., 2010, *Next Generation Nuclear Plant Steam Generator and Intermediate Heat Exchanger Materials Research and Development Plan*, INL/EXT-08-14107 Rev. 1, Idaho National Laboratory, Idaho Falls, Idaho.

ASTM-2368-10 (2017), *Standard Practice for Strain Controlled Thermomechanical Fatigue Testing,* ASTM International, West Conshohocken, PA, 2020, www.astm.org

Wang, Y., Jetter, R. I, and Sham, T.-L. (2024), *Experimental and Analytical Verification of Asme Section III, Division 5 Creep-Fatigue Design Rules, PVP2024-123351,* Proceedings of the ASME 2024 Pressure Vessel and Piping Conference, American Society of Mechanical Engineers, New York, NY.

Wang, Y., Jetter, R. I, Messner, M.C., and Sham, T.-L. (2018), *Report on FY18 Testing Results in Support of Integrated EPP-SMT Design Methods Development,* ORNL/TM-2018/887, Oak Ridge National Laboratory, Oak Ridge, Tennessee.